Fluctuations of Initial State and Event-by-Event Pseudo-Rapidity Correlations in High Energy Nuclear Collisions

Lebedev I.

Institute of Physics and Technology, Satbayev University, Almaty, Kazakhstan,
lebedev@sci.kz, lebedev692007@yandex.ru

According to the present-day conceptions, the hadron substance transits within the interactions of the nuclei, at the high energies, into a state of the quark-gluon plasma (QGP), in which the quarks and gluons stay in a quasi-free state.

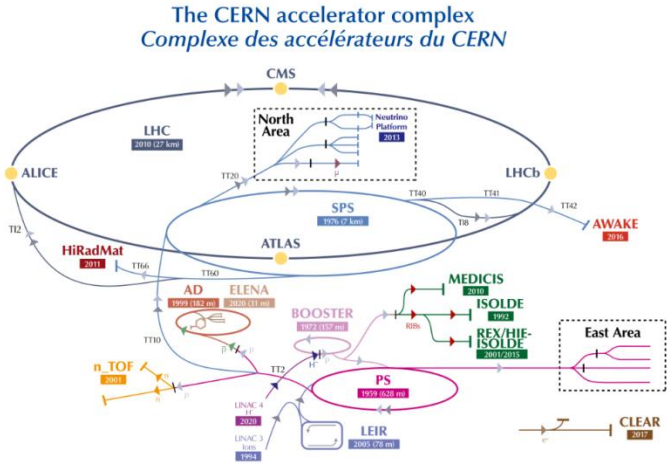

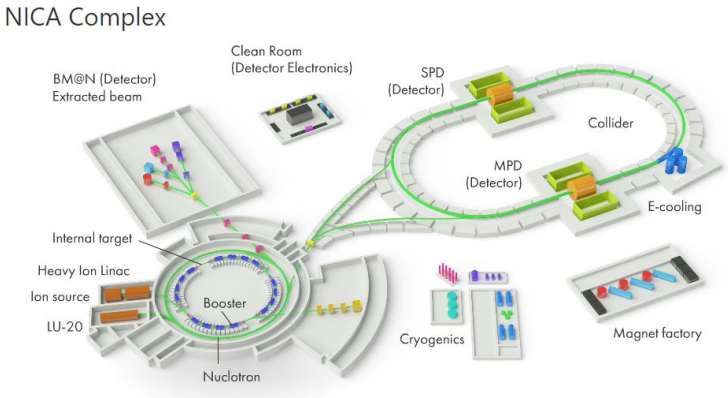

The study of quark-gluon plasma has mainly focused on two complementary directions.

The first direction is associated with studies of interactions of heavy ions at the maximum available energies.

The second direction is focused on the search for the critical point of the phase transition of hadronic matter into the QGP state. It is assumed to be in the energy range from several GeV to several tens of GeV. First, it is considered that the investigations nearby the critical point of the phase transition into the quark-gluon plasma will give a possibility to get the quality new results on the process dynamics. Second, according to the theoretical predictions, a mixed phase of the ‘excited hadronic matter’, which includes both the free quarks and gluons, and the protons with neutrons, must be formed within the range of the energies of 4 to 11 GeV per nucleon.

Experimental Details

The present analysis has been carried out with the data obtained from nuclear emulsion track detector. Stacks of NIKFI BR-2 emulsions have been exposed to 10.6 AGeV Au-197 beam at the BNL synchrotron (AGS).

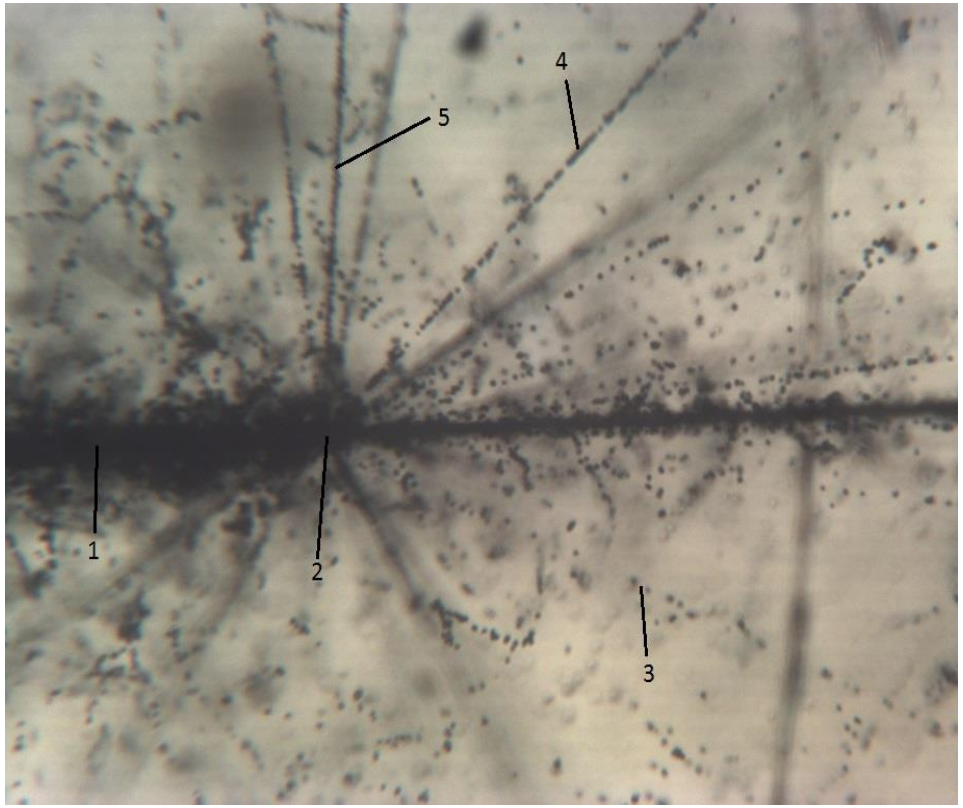

Figure 1 – Photo of the interaction of the gold nucleus with the emulsion nucleus at 10.6 AGeV. 1 - projectile nucleus; 2 - interaction center; 3 - s-particle; 4 - g-particle; 5 - b-particle.

All charged secondary particles were classified according to the commonly accepted emulsion experiment terminology into following groups:

Projectile fragments, including one-charge, two-charge and multi-charge one. The multiplicity of projectile fragments is denoted by N_f. For each projectile fragment, the charge was measured.

Target fragments, so-called *h*-particles, consisting of fast *g*-particles (one-charge target fragments with kinetic energy greater than 26 MeV) and slow *b*-particles (one-charge target fragments with kinetic energy less than 26 MeV or multi-charge target fragments). The multiplicity of target fragments is denoted by N_h.

Shower particles or relativistic singly charged particle, emitted from interactions area. The multiplicity of shower particles is denoted by n_s. The pseudo-rapidity ($\eta = -\ln[\tan\Theta/2]$) was calculated for each shower particle.

Collision Geometry Analysis

The geometry was estimated using the analysis of spectator fragments of colliding nuclei.

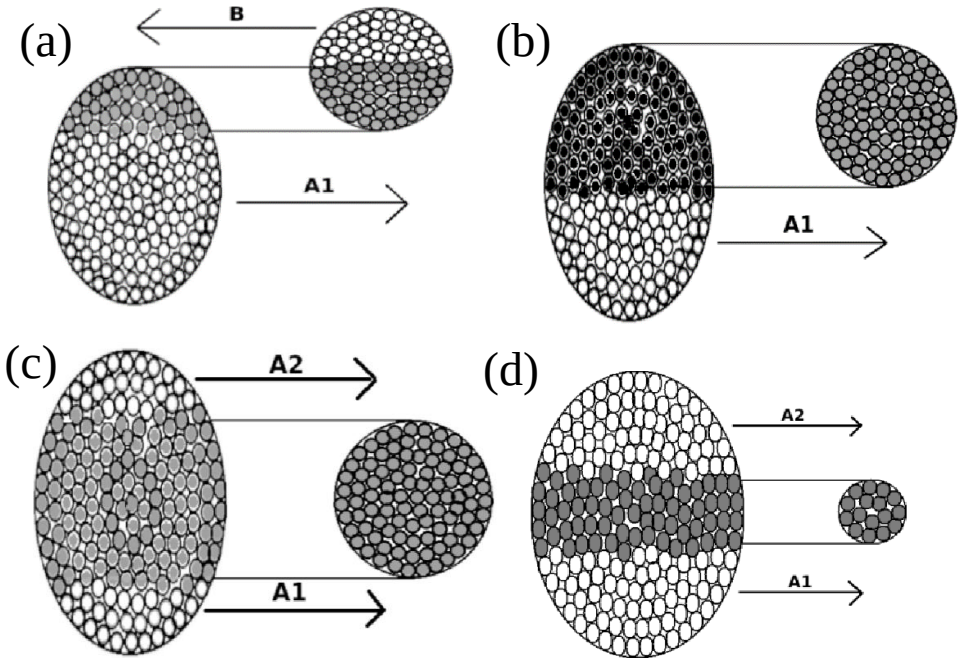

Figure 2 – Schematic representation of the interaction of nuclei with different degrees of centrality. Participating nucleons are marked in dark color (based on geometric representations). The light color indicates spectator nucleons that form fragments of the projectile and target nuclei.

Based on geometric concepts, it follows that in peripheral events one multi-charged fragment (A1) of the projectile-nucleus should be detected (Fig.2a). Moreover, its charge is the higher, the greater the degree of collision peripherality.

As well one multi-charged fragment (A1) of the projectile-nucleus should be detected in weakly central interactions (Fig.2b).

In strongly central interactions, there should be the highest probability of occurrence of events with two multi-charged fragments (A1, A2). In this case, the smaller the target-nucleus, the larger the charges of the fragments should be detected (Fig.2c, Fig.2d). For large targets, events of complete destruction (when there are no multi-charged fragments) of the projectile-nucleus can be observed.

Thus, depending on the collision geometry, a different number of multi-charged fragments is produced.

The NIKFI BR-2 emulsion includes hydrogen (39.2%), CNO nuclei (35.3%), and AgBr nuclei (25.5%). This makes it possible to analyze nuclear interactions of different degrees of asymmetry of nuclei under the same experimental conditions.

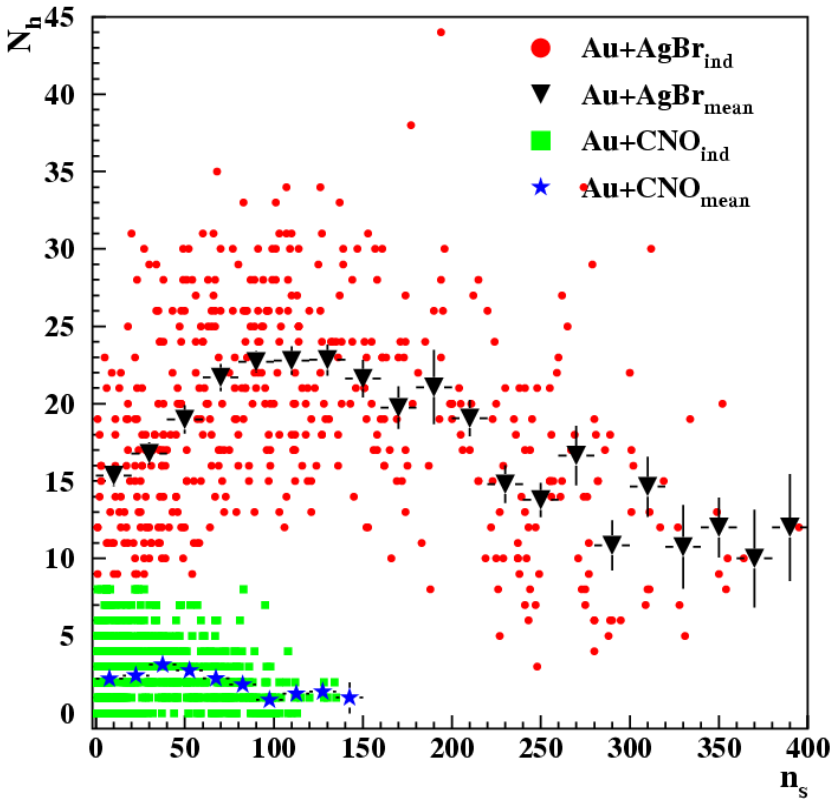

Figure 3 – Dependence of the total number of fragments of the target nucleus ($N_h=n_b+n_g$) and the number of shower particles n_s for the interaction of projectile-nucleus with heavy (AgBr) and light (CNO) target-nuclei.

The separation of events with different targets was carried out according to the following criteria.

First, the heaviest nucleus from CNO is oxygen with a charge equal to 8. Therefore, the number of fragments of the target-nucleus (N_h) cannot be more than 8. Second, the multiplicity of n_s in the interactions of gold with heavy nuclei (Au+AgBr) is much higher than with Au+CNO.

The maximum of the curve (N_h versus n_s) separates peripheral and central interactions.

The increase in the number of *h*-particles is associated with the fragmentation of multi-charged fragments of the target-nucleus. At a level approximately corresponding to $n_s \sim 110$ for Au+AgBr ($n_s \sim 45$ for Au+CNO), the target-nucleus is completely destroyed.
At $n_s > 110$, as the centrality of the interaction increases, the multiplicity of shower particles increases. In a strongly central collision, the number of shower particles is maximal, and the number of target-nucleus fragments is minimal.

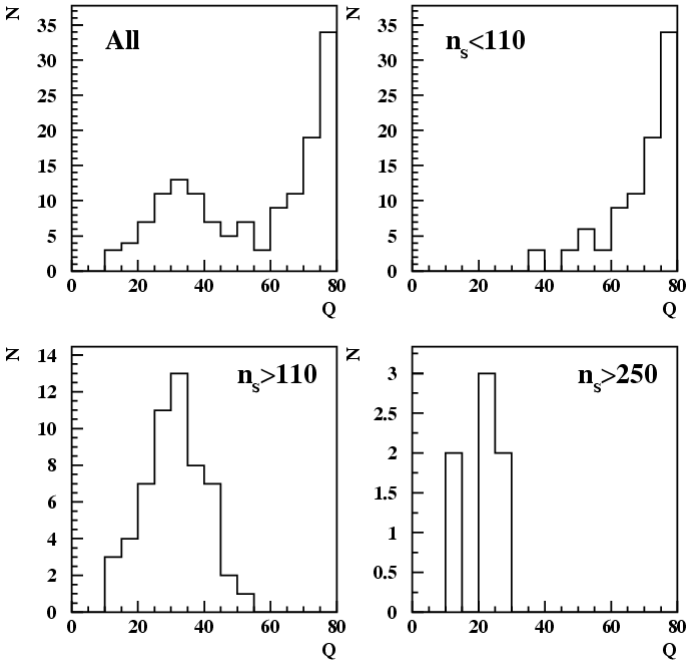

Figure 4 – Charge distribution of a multi-charged fragment of projectile-nucleus for the interaction of Au + AgBr with one multi-charged fragment N_f = 1 depending on the n_s multiplicity.

The total charge of fragments of the projectile nucleus is the higher, the greater the degree of peripherality of the collision.

The total distribution is characterized by two distinct peaks. The first peak is formed by events with $n_s < 110$, the second one by events with $n_s > 110$. Peripheral events of different degrees of peripherality characterize the peak in the region of large Q values. The peak at $Q < 55$ refers to central events and characterizes interactions with different degrees of centrality.

Thus, the character of fragmentation of projectile-nucleus does not change smoothly when passing from peripheral to weakly central interactions.

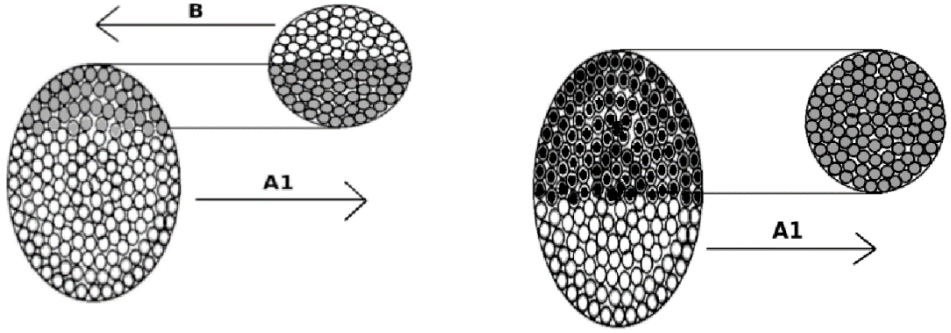

Fluctuations of the Average Pseudo-Rapidity in Event

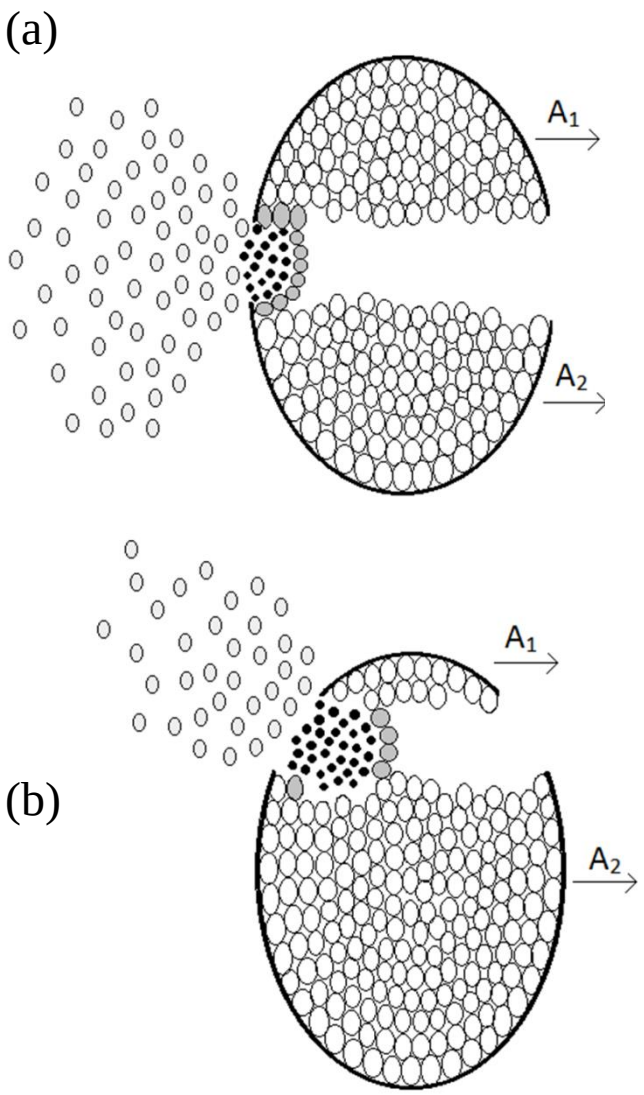

In strongly central and weakly central events, the resulting fireball is taken to different directions differently.

Thus, depending on the collision geometry, fluctuations of the average value of pseudo-rapidity distribution of secondary particles should be detected.

Figure 5 – (a) Strongly central and (b) weakly central events

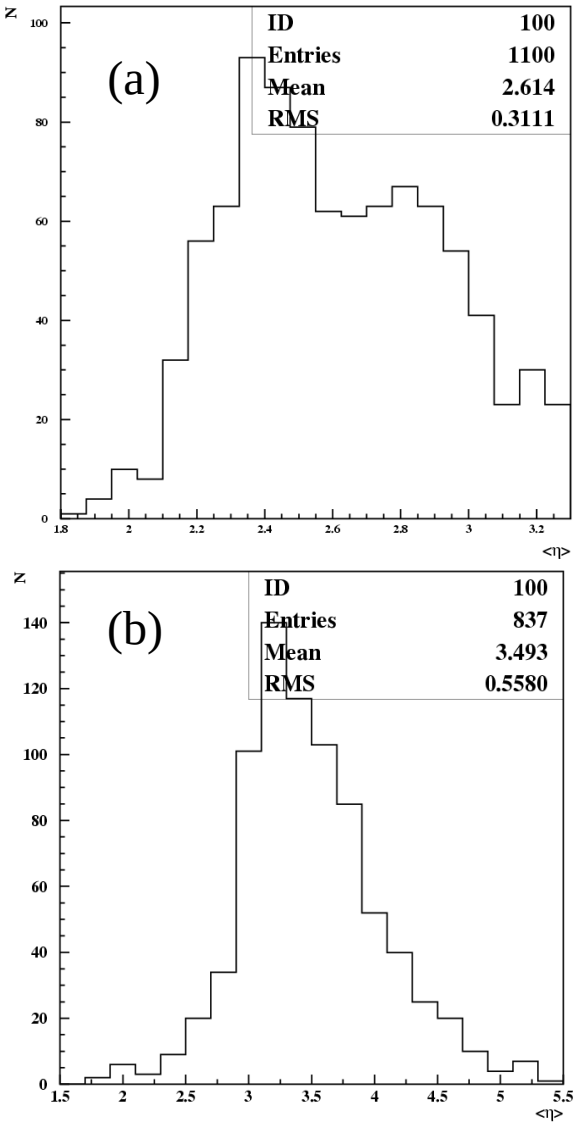

Figure 6 – The distribution of the average pseudo-rapidity in event of (a) Au + Em 10.6 AGeV and (b) Si + Em 14.6 AGeV.

To study these fluctuations in each event the average pseudo-rapidity $<\eta>$ was calculated to search for a possible deviation of the direction of emission of secondary particles due to the collision geometry or other reasons. Then the distribution of average pseudo-rapidity, calculated in each single event, was plotted.

The distribution of $<\eta>$ for Au + Em 10.6 AGeV is an asymmetric type. It looks like the two distributions with mean values of $<\eta> \sim 2.35$ and $<\eta> \sim 2.85$ overlap.

For comparison in Fig. 6b is shown the same distribution for experimental data Si + Em 14.6 AGeV.

In contract to Fig. 6a, the distribution $<\eta>$ for Si + Em 14.6 AGeV (Fig. 6b) does not have a characteristic bump in the region of large $<\eta>$.

To investigate this feature in more detail, we analyzed the pseudo-rapidity distributions of individual events, which have $<\eta>$ in the intervals from 2.3 to 2.4 and from 2.8 to 2.9, comparing them with each other.

Events from first interval have a Gaussian-like structure. The events from second interval (Fig. 7b) have a more complex structure compared to the events shown in Fig. 7a. In addition to the "standard" group of particles emitted with pseudo-rapidity $\eta \sim 2.35$, a significant part of particles have $\eta \sim 4$. Moreover, in some events, for example, with ID numbers $N_{ev} = 5513014$ and $N_{ev} = 11017$, the distribution looks like as a two-humped distribution (two groups of secondary particles are formed with significantly different pseudo-rapidity).

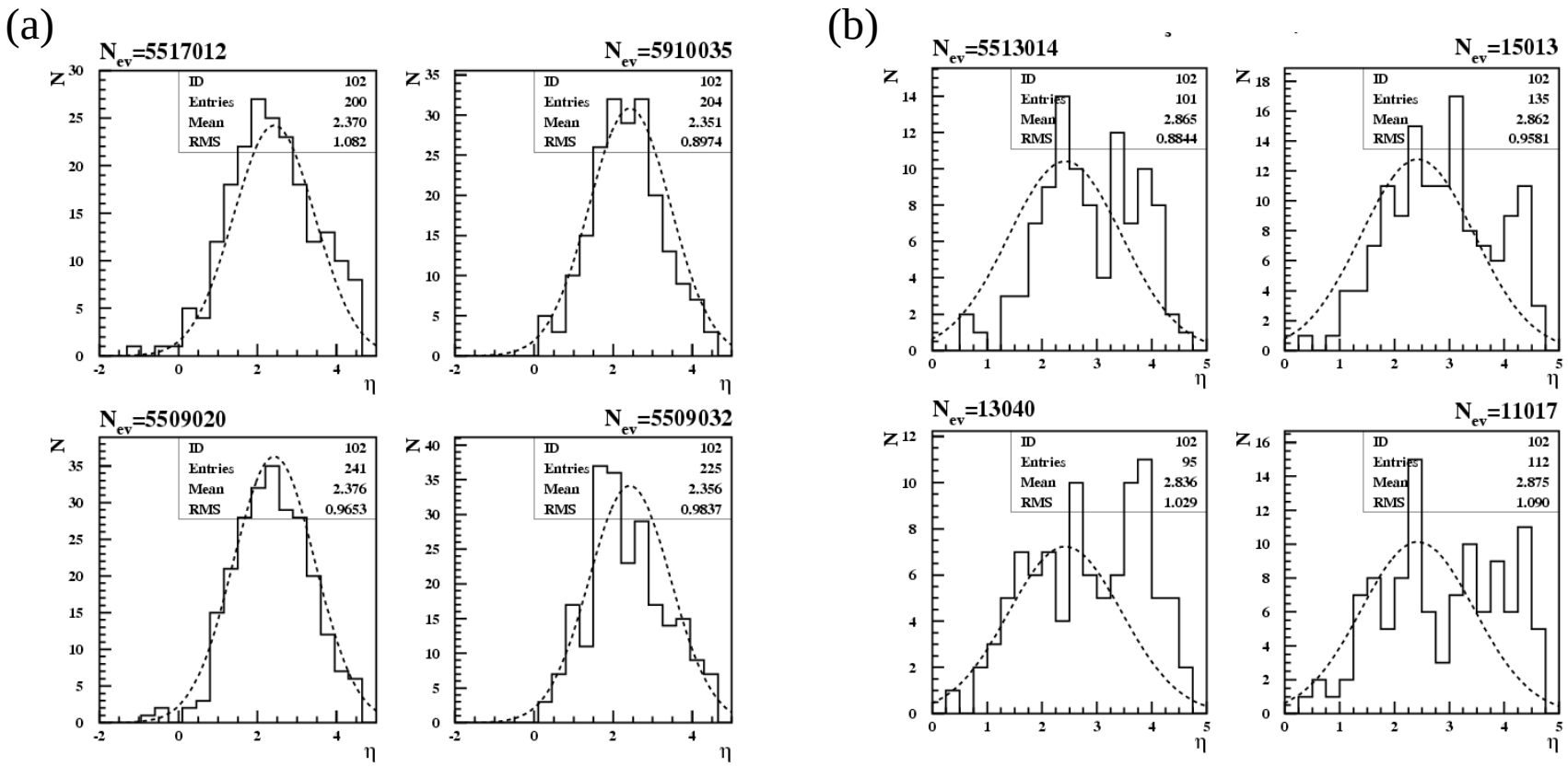

Figure 7 – Pseudo-rapidity distribution of individual events Au + Em 10.6 AGeV with the mean pseudo-rapidity in the intervals: (a) from 2.3 to 2.4 and (b) from 2.8 to 2.9. Solid lines are experimental pseudo-rapidity distributions. Dashed lines are fit of the event $N_{ev} = 5517012$ (normalized to the multiplicity).

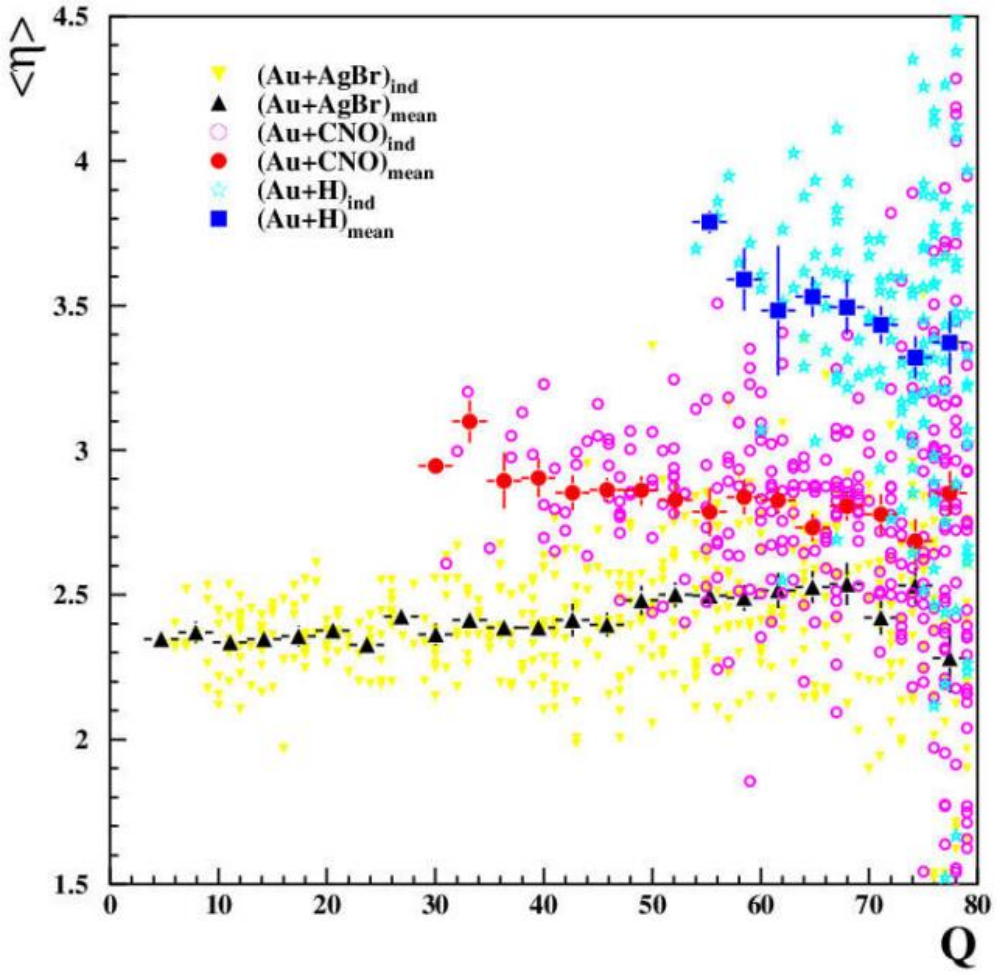

Figure 8 – Average values of the pseudo-rapidity distribution of *s*-particles as a function of the total charge of the projectile-nucleus Au-197 with heavy and light emulsion nuclei.

The average value of the pseudo-rapidity distribution of shower particles for the interactions of gold nuclei with CNO nuclei is located in the region $\langle\eta\rangle \sim 2.85$.

The average value of the pseudo-rapidity distribution of shower particles for interactions of gold nuclei with heavy AgBr nuclei is located in the region $\langle\eta\rangle \sim 2.35$.

It should be noted that for the central Au + CNO interactions of a higher degree of centrality, which are characterized by a lower value of the total charge of the residual fragments of the projectile nucleus, higher values of the average pseudo-rapidity are observed.

In Au + AgBr interactions, the opposite effect is observed: with an increase in the degree of centrality (that is, for interactions with a lower Q value) of the interaction, the average pseudo-rapidity decreases.

Pseudo-Rapidity Correlations

The search for correlated groups of secondary particles was carried out using the Hurst method.

The classical Hurst method was developed to analyze correlations in time sequences. If some analyzed sequence ξ_i is uncorrelated, the sum of fluctuations on a sufficiently large investigated interval of variation of the sequence ξ_i ($i >> 1$) will tend to zero. For a correlated signal $\Sigma(\xi_i - <\xi>)$ is significantly different from zero. To quantify the degree of correlation, two basic quantities are used: the standard deviation $S(k)$ and the so-called range $R(k)$. To calculate the range, the accumulated fluctuations $X(m, k)$ of the sequence are calculated relative to the average value $<\xi>$:

$$X(m,k) = \sum_{i=1}^{m} [\xi(z_i) - <\xi>], \qquad 1 \le i \le m \le k$$

$$R(k) = \underbrace{\max X(m,k)}_{1 \le m \le k} - \underbrace{\min X(m,k)}_{1 \le m \le k} \qquad <\xi> = \frac{1}{k}\sum_{i=1}^{k} \xi(z_i).$$

$$S(k) = \left[\frac{1}{k} \sum_{i=1}^{k} [\xi(z_i) - <\xi>]^2 \right]^{1/2}.$$

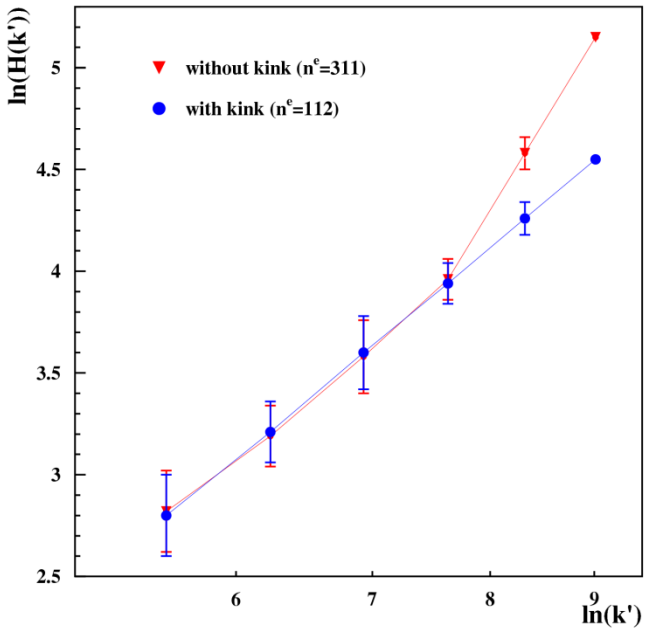

Figure 9 - Hurst curves for two characteristic events Au+Em 10.6 AGeV

The strength and length of correlations are estimated based on the following relationship:

$$H(k) = R(k) / S(k) \qquad H(k) = (ak)^h$$

The h parameter is the Hurst index. If the sequence is not correlated, then the correlation index (Hurst index) will be equal to 0.5. The strength of the signal correlation depends on the value of the Hurst index $0.5 \le h \le 1$. The higher the value of h, the more correlated the analyzed sequence is.

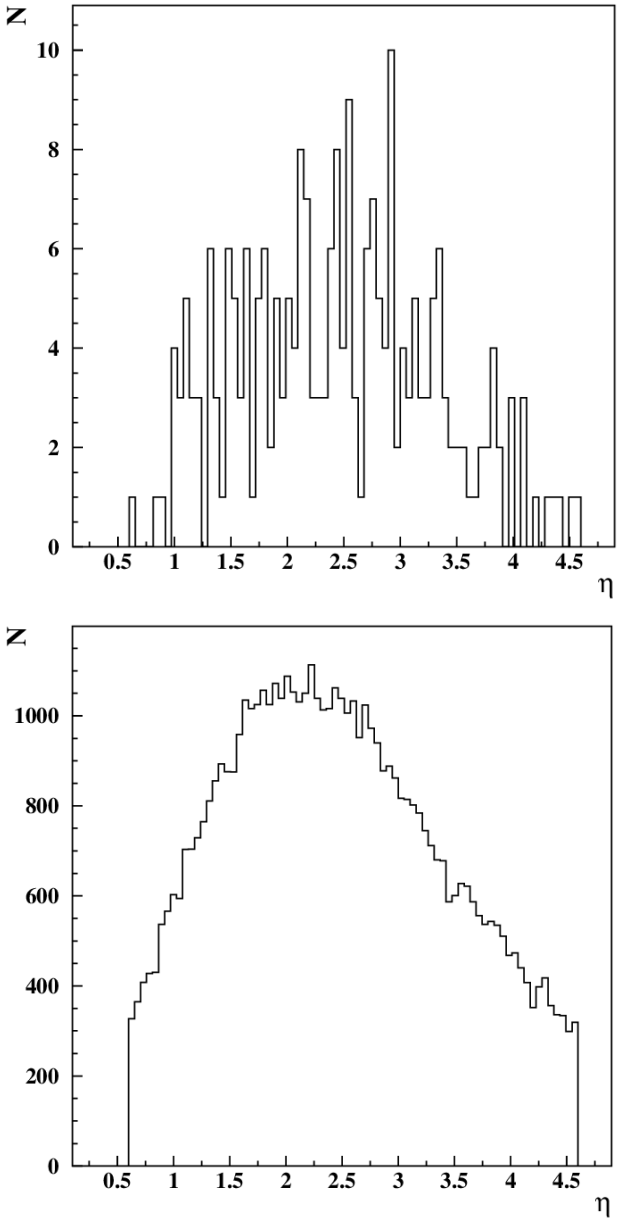

Figure 10 – Pseudo-rapidity distribution of Au+AgBr: a) individual event; b) all events

For the analysis, we used the central pseudo-rapidity interval from $\eta_{min} = 0.6$ to $\eta_{max} = 4.6$.
This pseudo-rapidity interval is divided into k = 1024 parts.
Fluctuations in an individual event relative to the total pseudo-rapidity distribution (normalized to the multiplicity) were analyzed in the following form:

$$\xi_i = \left(\frac{n_i^e}{n^e} - \frac{n_i}{n}\right) \Big/ \frac{n_i}{n}$$

n_i^e - the number of particles hitting i-th subinterval in individual event.
n_i^e - the multiplicity of the event.
n_i - the number of particles hitting i-th subinterval in the total pseudo-rapidity distribution .
n - the multiplicity of the total pseudo-rapidity distribution.

We calculated the normalized range $R(k)/S(k)$ corresponding to the length of the pseudo-rapidity interval $d\eta = 4$ (k=1024).
After that, the sequence ξi was split in half into two sequences. In each of these sequences, the normalized range $R(k)/S(k)$ was calculated. The value of the normalized range for these two parts was averaged and, thus, the normalized range corresponding to the length of the pseudo-rapidity interval $d\eta = 2$ (k=512) was calculated.
This procedure of dividing the pseudo-rapidity interval and calculating the normalized range continued until the number of sub-intervals became less than 16 ($d\eta = 0.0625$) , since the number of members of the analyzed sequence should be >>1.
The obtained values of the normalized range R/S, depending on the length of the pseudo-rapidity interval $d\eta$ were fitted using function $H(k) = (ak)^h$ to find the value of the Hurst index.

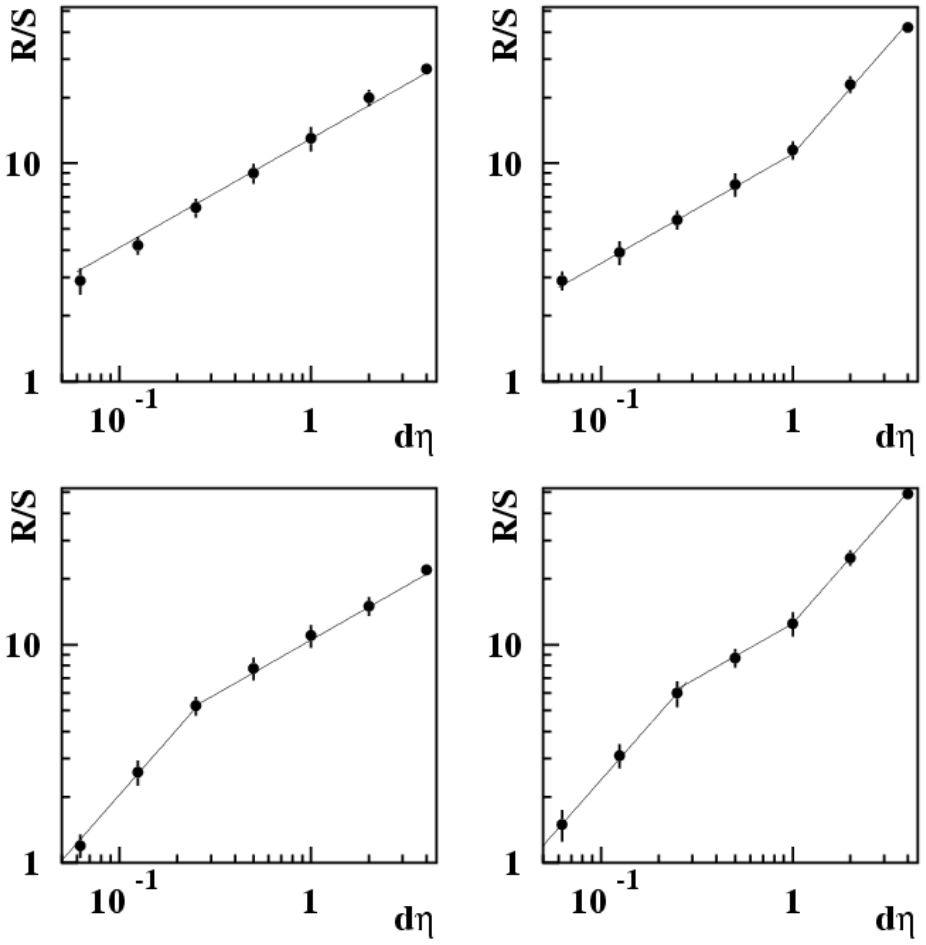

Figure 11 – The Hurst curve for four characteristic events

Based on the analysis of the behavior of the Hurst exponent, all events were divided into 4 types:

1. Events with linear behavior of the Hurst curve with exponent $h \sim 0.5$ (uncorrelated η-distributions)

2. Events with $h \sim 1$ at small pseudorapidity intervals ($d\eta < 0.25$) and $h \sim 0.5$ at $d\eta > 0.25$ (η-distributions with short-range correlations).

3. Events with $h \sim 1$ at large pseudorapidity intervals $d\eta > 1$ and $h \sim 0.5$ at $d\eta < 1$ (η-distributions with long-range correlations).

4. Events with $h \sim 1$ both at small and large pseudorapidity intervals, but $h \sim 0.5$ at medium pseudorapidity intervals $0.25 < d\eta < 1$ (mixed type events).

Events of various types differ significantly in the fragmentation of the projectile-nucleus, multiplicity of secondary particles and pseudo-rapidity distribution.

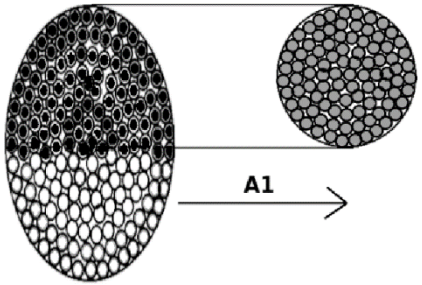

This behavior of the Hurst curve corresponds to short-range correlations in the pseudo-rapidity distributions. In most events with short-range correlations, one multi-charged fragment of the projectile nucleus was detected. Such events are most likely to be related to central interactions with a low degree of centrality.

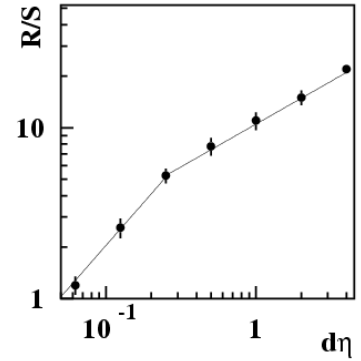

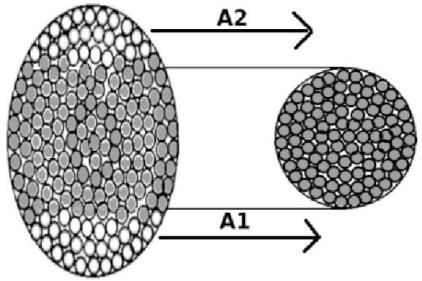

This behavior of the Hurst curve corresponds to long-range correlations in the pseudo-rapidity distributions. In most events of this type, the process of complete destruction of the projectile nucleus is observed, which is characterized by the absence of multi-charged fragments of the projectile. Events with long-range correlations have the high average multiplicity $<n_s>$ ~ 272. Such events mainly correspond to the central interactions of gold nuclei with heavy nuclei (AgBr) of the emulsion.

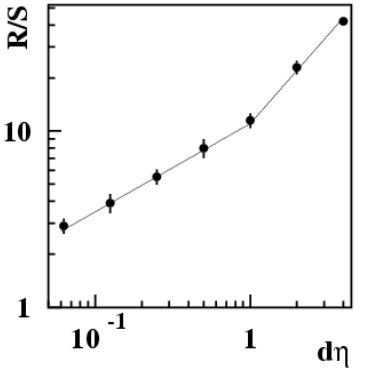

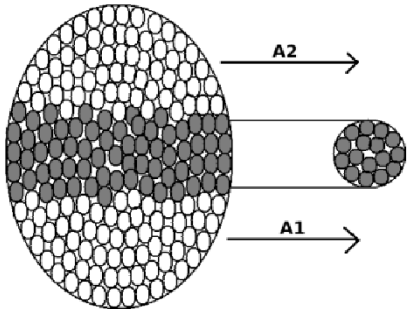

These events have several multi-charged fragments of projectile-nucleus and mean multiplicity $<n_s>$ ~ 97. They mainly correspond to central interactions of gold nuclei with light CNO nuclei of the emulsion. Events of mixed type have “anomalous” pseudo-rapidity distribution: two streams of secondary particles are formed with significantly different pseudo-rapidity.

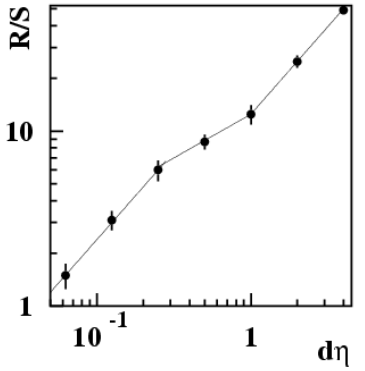

Conclusion

•In this presentation the joint study of fluctuations of initial state and event-by-event pseudo-rapidity correlations in relativistic nucleus-nucleus interactions is presented. The results were obtained on the basis of an analysis of experimental data obtained with a track detector (NIKFI BR-2) exposed to 10.6 AGeV Au-197 beam at the BNL synchrotron.

•Based on the analysis of the behavior of the Hurst index, the total ensemble of events has been divided into four types: uncorrelated, with short-range correlations, with long-range correlations and mixed type. Events of various types differ significantly in the fragmentation of the projectile-nucleus, multiplicity of secondary particles and pseudo-rapidity distribution.

•Events of mixed type have "anomalous" pseudo-rapidity distribution: two groups of secondary particles are formed with significantly different pseudo-rapidity. The events mainly correspond to central interactions of heavy Au nuclei with light CNO nuclei.

•The "anomalous" pseudo-rapidity distributions were not found in the interactions of medium Si nuclei with emulsion nuclei. The question of why the anomalous pseudo-rapidity distribution (found in Au+CNO interactions) is not observed in Si + CNO interactions requires careful study. This is probably due to the significantly different degree of asymmetry of the interacting nuclei.

Thank you for attention